Colloque SHF "*Prévision des crues et des inondations – Avancées, valorisation et perspectives*"
Toulouse, 28-30 novembre 2023

ASSIMILATION DE DONNÉES DE TÉLÉDÉTECTION DANS UN MODÈLE CHAINÉ HYDROLOGIE-HYDRAULIQUE POUR LES INONDATIONS

Remote Sensing Data Assimilation with a Chained Hydrological-hydraulic Model for flooding

NGUYEN Thanh Huy[1,2*], PIACENTINI Andrea[1], MUNIER Simon[3], RICCI Sophie[1,2], PENA LUQUE Santiago[4], RODRIGUEZ SUQUET Raquel[4], BONASSIES Quentin[1,2], FATRAS Christophe[5], LAVERGNE Emeric[5], ANDRAL Alice[5], BRUNATO Sylvain[6], GAUDISSART Vincent[6], GUZZONATTO Eric[6], VALLADEAU Guillaume[7], POISSON Jean-Christophe[7], FROIDEVAUX Alice[8], GUIOT Antoine[8], RAYNAL Romaine[8], HUYNH Thanh-Long[8], HUANG Thomas[9], KETTIG Peter[4], BLANCHET Gwendoline[4], BRETAR Frederic[4]

** auteur correspondant*
[1] CERFACS, 31057 Toulouse Cedex 1, France (e-mail: thnguyen@cerfacs.fr; piacentini.palm@gmail.com; ricci@cerfacs.fr; bonassies@cerfacs.fr)
[2] CECI, CNRS UMR 5318/CERFACS, 31057 Toulouse Cedex 1, France
[3] CNRM, 31057 Toulouse Cedex 1, France (e-mail: simon.munier@meteo.fr)
[4] CNES, 31401 Toulouse Cedex 9, France (e-mail: raquel.rodriguezsuquet@cnes.fr; santiago.penaluque@cnes.fr; peter.kettig@cnes.fr; gwendoline.blanchet@cnes.fr; frederic.bretar@cnes.fr)
[5] CLS, 11 rue Hermès, Parc Technologique du Canal, 31520 Ramonville Saint-Agne, France (e-mail: cfatras@groupcls.com; elavergne@groupcls.com; aandral@groupcls.com)
[6] CS Group, 31500 Toulouse, France, France (e-mail: sylvain.brunato@csgroup.eu; vincent.gaudissart@csgroup.eu; eric.guzzonato@csgroup.eu)
[7] VorteX.io, 31401 Toulouse Cedex 9, France (e-mail: guillaume@vortex-io.fr; jeanchristophe@vortex-io.fr)
[8] QuantCube Technology, 75002 Paris, France (e-mail: a.froidevaux@quant-cube.com; a.guiot@quant-cube.com; r.raynal@quant-cube.com; thanh-long.huynh@quant-cube.com)
[9] NASA Jet Propulsion Laboratory, California Institute of Technology, Pasadena, CA, USA (thomas.huang@jpl.nasa.gov)

Choix du thème/session : 2/ Prévision des crues et des inondations

Résumé:
La gestion efficace du risque d'inondation repose sur des prévisions fiables à des échéances suffisamment longues pour permettre la mise en œuvre de mesures de protection efficaces. Un modèle chaîné hydrologique-hydraulique est implémenté ici, utilisant les prévisions de débit d'un modèle hydrologique à grande échelle, notamment ISBA-CTRIP comme des conditions aux limites d'un modèle hydrodynamique local et à haute fidélité. Dans ce travail, les incertitudes associées au forçage hydrologique provenant d'ISBA-CTRIP et aux paramètres hydrauliques de frottement sont réduites à l'aide d'un filtre de Kalman d'ensemble, implémenté sur le solveur hydraulique TELEMAC-2D. L'algorithme d'assimilation des données assimile conjointement les mesures de niveaux d'eau in-situ et les masques d'eau obtenus à partir d'observations satellitaires. Les masques d'eau dérivés des images radar à synthèse d'ouverture (RSO, ou SAR en anglais) sont exprimées en termes de ratios de surfaces inondées sur des sous-domaines de la plaine inondable, ce qui permet de corriger l'état hydraulique dans les plaines d'inondations particulièrement au pic de crue et pendant la décrue. La non-gaussianité des erreurs de ces observations est traitée avec une fonction d'anamorphose gaussienne afin de garantir l'optimalité de l'EnKF. Cette stratégie d'assimilation conduit à l'amélioration des métriques 1D et 2D, i.e. une réduction du RMSE et une augmentation de l'indice CSI dans les plaines d'inondation. L'algorithme d'assimilation corrige le frottement et le forçage de sorte que l'état hydraulique simulé dans le lit de la rivière et dans les plaines d'inondation soit cohérent avec les observations, ce qui permet d'établir une ré-analyse des épisodes d'inondation. Ce travail démontre que, bien qu'imparfait, le forçage hydrologique peut être utilisé comme condition limite du modèle hydraulique et que l'assimilation des données permet une réduction efficace de l'incertitude sur ces forçages. Ces conclusions justifient une assimilation de données hétérogènes au sein d'un modèle multi-physique

hydrologique-hydraulique dans le but d'allonger l'échéance de prévision, ainsi qu'une modélisation hydrodynamique sur des bassins non jaugés.

Mots clefs: Modélisation hydrodynamique, surfaces inondées, couplage multi-physiques, télédétection, assimilation de données.

Abstract:
Effective flood risk management involves reliable forecasts at extended lead times as this allows for the implementation of cost-effective and socially acceptable measures. A chained hydrologic-hydraulic model is implemented here, using large-scale hydrologic model's (namely ISBA-CTRIP) discharge forecasts as inputs to local and high-fidelity hydrodynamic models. In the present study, uncertainties in the hydrologic forcing from ISBA-CTRIP, as well as in hydraulic parameters, are reduced with an EnKF implemented on the TELEMAC-2D solver. The data assimilation algorithm jointly assimilates in-situ water level measurements and water masks obtained from satellite Earth Observations. The SAR-derived binary wet/dry maps are expressed in terms of wet surface ratios (WSR) over selected subdomains of the floodplain. This allows to correct the hydraulic state in the flood plain at flood peak and during recess. The non-Gaussianity of the errors in the WSR observations are dealt with a Gaussian anamorphosis function. The chained data assimilation strategy leads to a significant improvement of the 1D and 2D metrics, with reduced RMSE and increased Critical Success Index. The assimilation algorithm corrects friction and forcing so that the simulated hydraulic state in the river bed and in the floodplains is consistent with the observations, which provides a reliable re-analysis of the past flood events. This work demonstrates that, while imperfect, forcing provided by a hydrology model can be efficiently used as input to a local hydraulic model, and that DA allows for an efficient reduction of the uncertainty in the hydrology products. These conclusions advocate for a heterogeneous data assimilation strategy implemented on top of a chained multiphysics hydrology-hydraulic model favorable to extended lead time forecasts, as well as for a modeling in ungauged catchments.

Key words: Hydrodynamic model, Flood extent, Multiphysics coupling, Remote sensing, Data assimilation

1. Introduction

Early warning and prediction of flood events have become all the more essential as the occurrence and intensity of flooding have increased in recent decades, especially in the context of climate change (EMDAT, 2021). In the context of operational flood forecasting, the challenges lie in producing reliable forecasts given constrained computational resources within processing times that should be compatible with operational forecasting. Hydrodynamic or hydraulic models—which are fundamental to estimate water level and flood extents—require observed data from stream gauge networks. Water level and/or discharge are prescribed as forcing time-series at the upstream and lateral boundary conditions (BCs) of the models. However, such information is not always available, either due to a lack of in-situ gauge data or because the measurements acquired during high overflowing events are unreliable. Additionally, constraining the hydraulic model with the BCs that only originate from observed forcing time-series limits the lead time of its forecast capability under the transfer time of the river network. In order to reach longer forecast lead times, a forecasted inflow should be prescribed to the hydrodynamics model, for instance, using discharge simulated by large-scale hydrologic models. Due to their coarse resolution and simplification of physical processes, large scale hydrology models provide an uncertain forcing to hydrodynamic models, thus resulting in inaccurate predictions for flooding. Large scale hydrology outputs should thus be improved, for instance assimilating hydraulic variables in hydrodynamic models. The corrected forcings are then used to better represent the flood dynamics in re-analysis or forecast mode.

Flood simulation and forecast capabilities have been greatly improved thanks to advances in data assimilation (DA). DA combines observations as they become available with numerical models to reduce the uncertainties in the model state, parameters and/or boundary conditions.

A classical DA approach stands in the assimilation of water surface elevation (WSE) data, either from in-situ gauge measurements, from altimetry satellites, or retrieved from remote-sensing RS images using flood edge location information combined with complementary Digital Elevation Model data (Grimaldi *et al.*, 2016, Garambois *et al.*, 2002, Dasgupta *et al.*, 2021). Satellite radar data is particularly advantageous in flood studies, as it allows an all-weather day-and-night global-coverage imagery of continental water, which is depicted by low backscatter values resulting from the specular reflection of the incident radar pulses (Martinis *et al.*, 2015). Many research works have proposed the assimilation of RS-derived WSE as summarized in Revilla *et al.*, 2016. The need to retrieve WSE from flood extents can be avoided with a direct assimilation of SAR-derived flood probability maps (Hostache *et al.*, 2018) or even flood extent maps (Nguyen *et al.*, 2022).

In the present paper, the 2D flood extent observations derived from remote sensing images, namely Sentinel-1 Synthetic Aperture Radar (SAR) images, are assimilated jointly with in-situ water level observations, with an Ensemble Kalman Filter (EnKF). The DA algorithm reduces the uncertainties in the hydrodynamics (T2D) model parameters as well as in the forcing inputs provided by a large scale hydrology model (ISBA-CTRIP). This allows to improve the representation of the flooding when the local hydrodynamic model is forced by hydrology discharge time series.

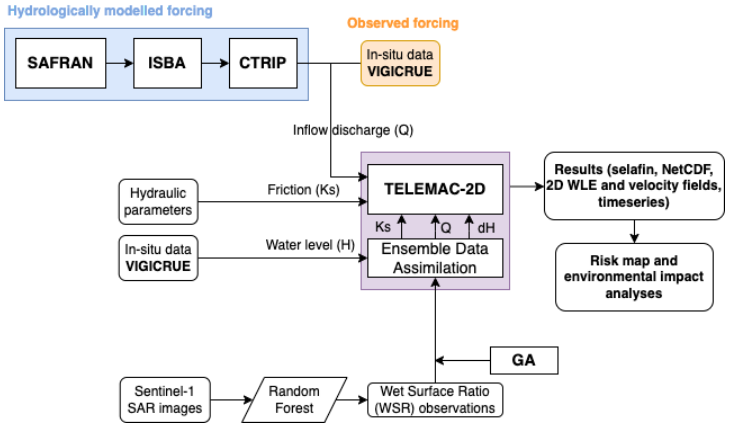

Figure 1: Workflow of the chained hydrologic-hydraulic model and the proposed DA strategy.

2. Models And Data

2.1 Hydrology and hydrodynamics models:

In the present work, the BC for a local-scale and high-fidelity hydrodynamic model with TELEMAC-2D (T2D, www.opentelemac.org) is provided by the large-scale hydrologic model ISBA-CTRIP (Munier and Decharme, 2022; Decharme *et al.*, 2019).

The general workflow for this strategy is displayed in Figure 1. As aforementioned, the chained multi-physics and multi-scales modeling approach involves a direct supply of discharge forcing data for the T2D hydraulic model by a hydrologic model (blue block in Figure 1), as an alternative of an observed streamflow from an in-situ gauging station (orange block in Figure 1). The ISBA-CTRIP hydrologic model results from the coupling of the ISBA land surface model (LSM) (Noilhan and Planton, 1989) and a CNRM-modified version of the TRIP river routing model (RRM) (Oki and Sud, 1998). LSMs simulate the energy and water balance at the soil-atmosphere-vegetation interface, while RRMs emulate the lateral transfer of freshwater towards the continent-ocean interface. The ISBA

model is defined at global scale on a 0.5°×0.5° regular grid that establishes the energy and water budget over continental surfaces, considering a three-layer soil. It provides a diagnostic of the surface runoff and the gravitational drainage, later used as forcing inputs for CTRIP. The CTRIP model is defined on a regular latitude-longitude grid at the 1/12° resolution and follows a river network to transfer water laterally from one cell to another, down to the interface with the ocean. This present work is based on the recent CTRIP version from (Decharme *et al.*, 2019; Decharme *et al.*, 2012) that provides a gridded map of discharge, illustrated in Figure 2 over France on 15/12/2020. The uncertainties in these simulated discharges mainly stems from uncertainties in the LSM inputs (i.e. precipitation), RRM parameters and catchment description.

2.2 Study area:

The study area is shown in Figure 3, it extends over a 50-km reach of the Garonne River between Tonneins and La Réole (rectangle in Figure 2). Observing stations, operated by the HydroFrance service and used for the VigiCrue platform, located at Tonneins, Marmande, and La Réole (black circles in Figure 3) provide water-level measurements every 5 to 15 minutes. The local T2D hydraulic model over this reach was developed by EDF and presented in (Nguyen *et al.*, 2022a). The Strickler friction coefficient Ks_k is assumed to be uniform over each of six segments of the river bed (with $k \in [1, 6]$, indicated by solid-colored segments, and also uniform in the entire floodplain (Ks_0). In addition, the limited number of in-situ observations yields errors in the formulation of the rating curve that is used to translate the observed water level into discharge, especially for high flow that would involve an extrapolation beyond the typically gauged values. In the present study, the discharge time-series at Tonneins, i.e. the forcing data for the T2D model, is either provided by gauge observations or CTRIP simulation, both highly prone to uncertainties, even though the two forcing data present different orders of magnitude.

It is worth noting that the hydrologic model ISBA-CTRIP generally yields better performances for large basins, and that a moderate performance is expected for the medium-sized Garonne catchment near Marmande, especially at high flows. Indeed, for major flood events, such a model tends to underestimate the discharge. Figure 4 shows CTRIP-simulated discharge at Tonneins (blue) along with the observed discharges (orange) for the two recent major flooding events that occurred in 2019 and 2021 (the time of acquisition of Sentinel-1/-2 images are indicated by vertical dashed lines). These time-series reveal that CTRIP underestimates the flood peaks—almost half of the observed peak discharge—and that such imperfection shall be accounted for with data assimilation of water-level in-situ observations and RS-derived flood extent observations.

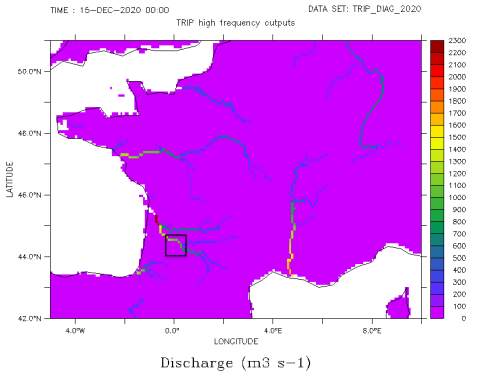

Figure 2: Discharge (m^3/s) simulated by CTRIP over France and neighboring countries on 15/12/2020.

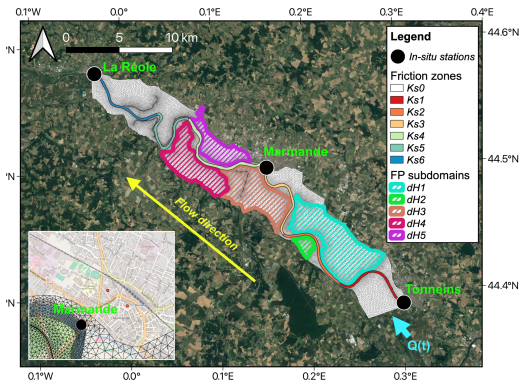

Figure 3: TELEMAC-2D Garonne Marmandaise domain (Nguyen et al., 2022b).

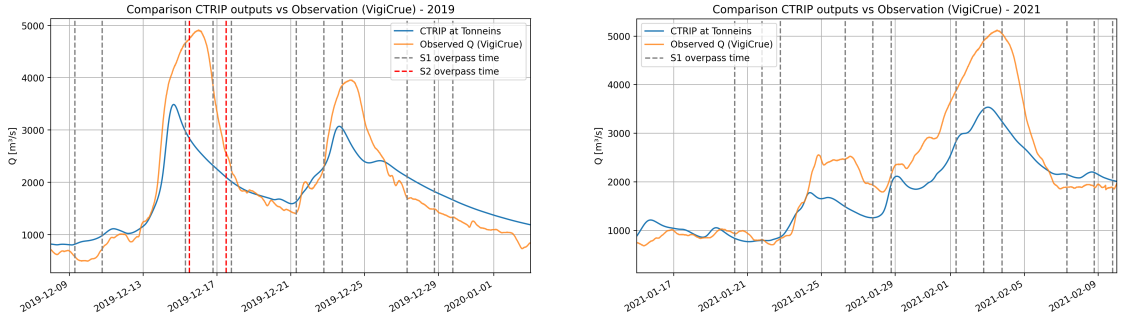

Figure 4: Hourly discharge time-series at Tonneins for the 2019 (left) and 2021 (right) flood events from VigiCrue gauge station (orange line) and simulated by CTRIP (blue line). The dates for Sentinel-1 images are indicated with vertical dashed lines.

3. Data Assimilation

The proposed DA strategy is a follow up of (Nguyen *et al.*, 2022a; Nguyen *et al.*, 2022b). The DA strategy is similar to that presented in (Nguyen *et al.*, 2023), here extended to account for the forcing data provided by the ISBA-CTRIP hydrologic model. Indeed, it is assumed that the major sources of uncertainties in the chained hydrologic-hydraulic model lie in the CTRIP-simulated hydrographs (that themselves stem from the input precipitation and uncertain LSM related to the run-off), in T2D friction parameters as well as in the simulated hydraulic state in the floodplain. Thus the errors in the CTRIP forcing are accounted for by a multiplicative factor μ applied on the discharge time-series. This corrective factor is constant over a DA cycle and varies between the DA cycles. In addition, the error in the hydraulic state that is due to the lack of evapotranspiration and ground infiltration (in the T2D hydraulic model) is taken into account as a correction of the water level dH_k (with $k \in [1, 5]$) over five selected subdomains of the floodplain, represented by the hashed regions in Figure 3. Within each of these floodplain subdomains, the hydraulic state correction is carried out uniformly, i.e. equal value for every node of the mesh that belongs to the same subdomain. The control space for DA thus gathered 4 friction coefficients, 1 multiplicative factor for the forcing and 5 uniform correction to the hydraulic state in the floodplain. In addition to in-situ water level measurements, the EnKF—involves 75 members with perturbed control parameters following Gaussian distributions—also assimilates the wet surface ratios (WSR) computed over these selected floodplain subdomains. This ratio stems directly from water masks derived from SAR images processed by a Random Forest algorithm from Sentinel 1 images. It is the ratio between the number of wet pixels in the subdomain and the total number of pixels in the subdomain. Moreover, the uncertainty reduction thanks to a dual state-parameter sequential correction by an EnKF is also enhanced with a Gaussian anamorphosis (GA) (Simon and Bertino, 2012). This GA algorithm allows us to deal with non-Gaussian errors associated with WSR observations by mapping these non-Gaussian quantities onto a Gaussian space. This favors the preservation of the optimality of the performed EnKF. In summary, the water level time-series at the three VigiCrue stations (i.e., Tonneins, Marmande and La Réole) and the WSR computed over the five floodplain subdomains, are assimilated with the EnKF algorithm implemented on the T2D Garonne Marmandaise model. This allows for a sequential correction of the friction, the inflow discharge, and water elevation in the floodplain subdomains. The EnKF algorithm is favoured in this work, as it allows to stochastically estimate the covariance matrices between the model inputs/parameters and outputs, without formulating the tangent linear of the hydrodynamics model.

4. Results

Three types of experiment are carried out for the 2021 flood event over the studied Garonne Marmandaise catchment: a free run (FR) without assimilation, also known as open-loop, a DA experiment (named IDA) that assimilates only in-situ water-level and a DA experiment (named IGDA) that assimilates both in-situ water-level and remote-sensing WSR observations. It should be noted that the 2021 event was not used for model calibration. Each simulation is achieved using measured forcing at Tonneins from VigiCrue (experiments denoted by FR^V, IDA^V and $IGDA^V$) or CTRIP forcing (experiments denoted FR^C, IDA^C, and $IGDA^C$). The simulation results are first assessed in the control space, then in the observation space using 1D and 2D metrics. In 1D assessment, the RMSE between observed and simulated water level at in-situ observing stations is computed to assess the dynamics of the flow in the river bed. On the other hand, in the 2D assessment, the agreements between flood extents simulated with T2D and flood extents derived from Sentinel-1 images are shown with a contingency map and an overall Critical Success Index (CSI) to assess the dynamics of the flow in the floodplains.

a. Result in the control space

Figure 5 shows the analyzed parameters from the different DA experiments, with solid orange and blue lines representing the mean of the analysis for $IGDA^V$ and $IGDA^C$, respectively, for the 2021 flood event. The shaded envelopes around each parameter line represent the standard deviation of the ensemble. The background standard deviation envelope is represented in opaque colors and overlapped by the analysis envelope in transparent color. The calibrated or default values are indicated by horizontal dashed lines in each panel, whereas the overpass times of Sentinel-1 over the 2021 flood event are indicated by vertical dashed lines. The analyzed values for the friction coefficients Ks_k (with $k \in [0, 6]$) are shown on the left column of Figure 5, while that of the inflow multiplicative correction μ is shown on the top panel of the right column. Next, the analyzed values of the hydraulic state correction dH_k (with $k \in [1, 5]$) in the DA experiments are shown on the remaining panels of the right column (with 0 for the default value). Lastly, the bottom right panel displays the reconstructed upstream discharges using the mean of the μ analysis for the ensemble.

First and foremost, the DA analysis for $IGDA^V$ and $IGDA^C$ provides corrections to the friction coefficients of the river bed that are quite similar in general (except Ks_1). Yet, the analyses for the friction in the floodplain Ks_0 and the correction to the inflow at Tonneins are very different. Indeed, CTRIP-simulated discharge is significantly underpredicted compared to the observed discharge, and leads to low water levels in the whole catchment without DA (as shown below in Figure 7). As a consequence, the EnKF prescribes a multiplicative factor $\mu>1$ to account for this lack of discharge, especially during the high flow between 2021-01-23 and 2021-02-06. Since the velocity in the floodplain is quite small, the friction coefficient in the floodplain (Ks_0) is not the most efficient control to drive the dynamics of the flow. This leads to small correction of Ks_0 for $IGDA^V$ compared to the calibrated value of 17 [$m^{1/3}.s^{-1}$] over the floodplain. Yet, when the misfit to the observations is large (i.e. when T2D is forced with the underestimated CTRIP discharge) the correction to Ks_0 becomes significantly different. For $IGDA^C$, the EnKF leads to smaller Ks_0 values than the default values (horizontal dashed lines). This increase of the friction acts as a mechanism to retain water within the zone, resulting in higher water levels than what were allowed for with the CTRIP discharge and the calibrated value of Ks_0. Both these effects are reversed during the flood recess when T2D struggles to empty the floodplain after the flood peak due to the absence of ground infiltration and evapotranspiration process in the model. On the other hand, the analysis for friction coefficients in the river bed are fairly similar between $IGDA^V$ and $IGDA^C$. Despite some equifinality issues, all of the friction coefficients remain within physical ranges.

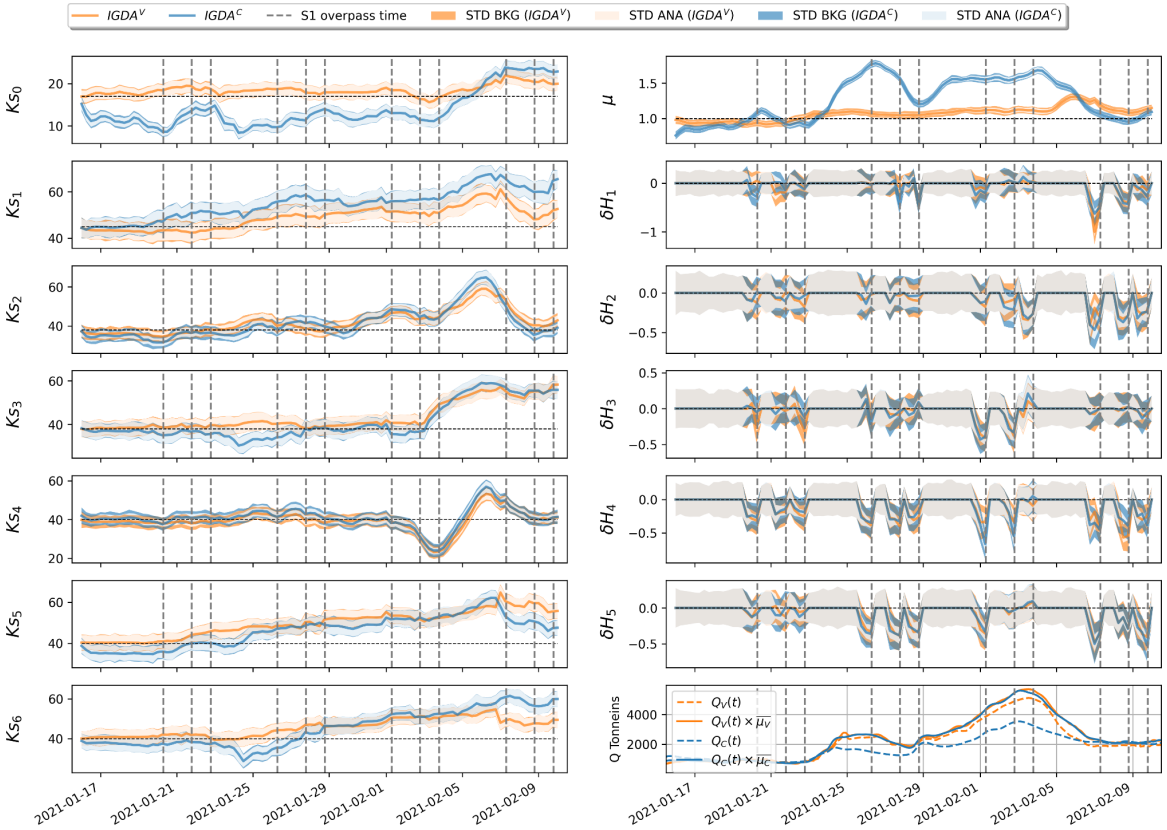

Figure 5: DA analysis (IGDA) for 2021 flood event, in the control space for friction coefficient Ks_0 in the floodplain (left column, top panel), $Ks_{[1, \ldots 6]}$ in the river bed (left column), multiplicative coefficient μ for inflow discharge at Tonneins (right column, top panel), uniform water level correction dH_k (with k ∈ [1, 5], right column) and reconstructed inflow discharges at Tonneins (right column, bottom panel).

The hydraulic state corrections dH_k (with k ∈ [1, 5]) are shown with non-null values at each S1 overpass, and for the most part, they are negative corrections (i.e. a water removal) to enhance the evacuation of water after the flood peaks. The standard deviations for dH_k are reduced by the analysis as shown by the background envelope being much larger than the analysis envelope. The reconstructed hydrograph at Tonneins, shown in the last panel on the right column, for $IGDA^C$ (blue line) is close to that of $IGDA^V$ (orange line) which illustrates that the EnKF succeeds in retrieving a realistic forcing time series even when the a priori hydrograph is significantly underestimated (shown by the blue dashed line compared to the orange one).

b. Results in the observation space with 1D metrics on water levels at observing stations

Figure 6 shows the water levels at the observing stations at Tonneins (red), Marmande (blue) and La Réole (green) simulated by FR^V (top panel) and $IGDA^V$ (bottom panel) compared to the observed water levels (plotted in respective black-dashed lines), for experiments forced by VigiCrue time-series. For $IGDA^V$, the ensemble of analysis is plotted in gray and the mean of the analysis is plotted in color. This result shows the efficiency of the DA strategy, including the performed EnKF, which is enhanced by the dual state-parameter estimation, and the GA.

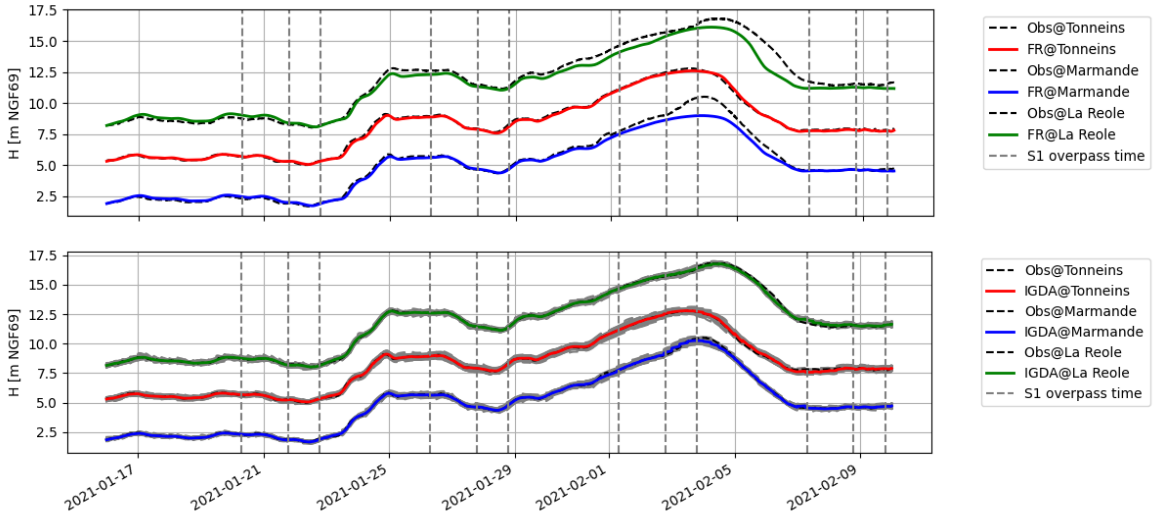

Figure 6: Water levels at the observing stations at Tonneins (red), Marmande (blue) and La Réole (green) simulated by FR^V (top panel) and $IGDA^V$ (bottom panel), compared to the observed water levels (plotted in black-dashed lines), for experiments forced by VigiCrue discharge.

Figure 7 is similar to Figure 6 but for the experiments forced by CTRIP discharge, instead of the observed discharge, to demonstrate the performance of the proposed DA strategy against even more extreme uncertainty. It was shown above in Figure 6 that the water levels stimulated by FR^V are slightly underestimated especially around the flood peak. Such an underestimation is all the more visible for the simulation forced by CTRIP discharge in Figure 7. Indeed, underestimated CTRIP discharge time-series leads to a significant underestimation at every high-water period, including the flood peak in FR^C, as shown in Figure 7. Both DA experiments lead to significant correction on the control leading to improved water levels at all three observing stations and over the entire event. This illustrates how DA allows for improved simulated water levels in the river, even when the input forcing is only a coarse approximation of the real inflow. It should be noted that the CTRIP discharge was significantly underestimated during the 2021 flood event, with a peak discharge predicted around 3,500 m^3/s compared to an observed discharge of 5,100 m^3/s.

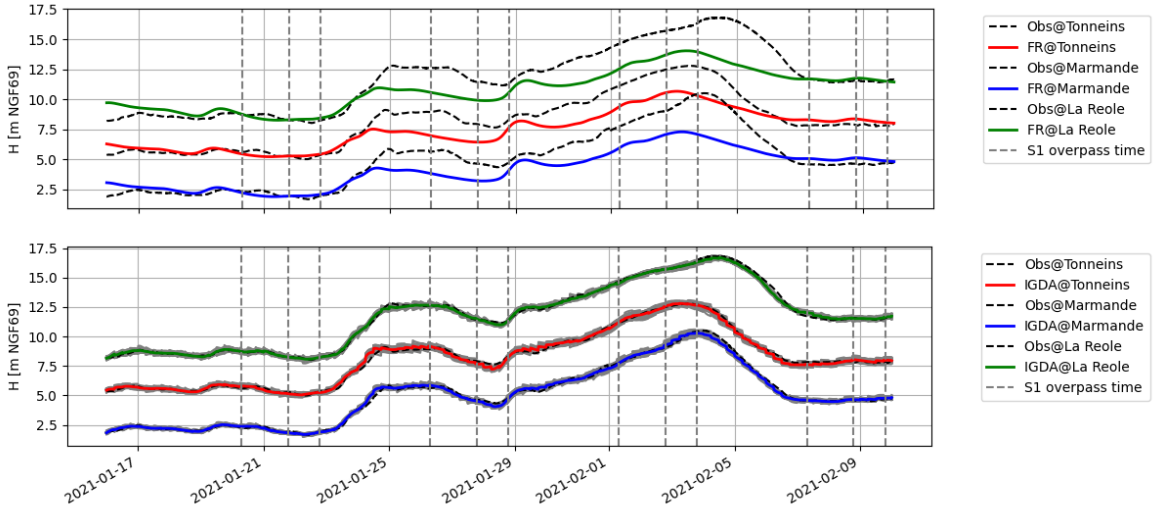

Figure 7: Water levels at the observing stations at Tonneins (red), Marmande (blue) and La Réole (green) simulated by FR^C (top panel) and $IGDA^C$ (bottom panel), compared to the observed water levels (plotted in black-dashed lines), for experiments forced by CTRIP discharge.

Table 1 summarizes the 1D quantitative results for all six experiments. The RMSEs between the simulated and the observed water levels at each observing station, as shown in Figure 6 and 7 for IGDA, are computed over time for the entire 2021 flood event. Coherent to the water level plots displayed above, the RMSEs underline the underestimation problem when CTRIP upstream forcings are used without DA, resulting in errors greater than 1 meter, which are critical regarding flood hazard assessments. Moreover, for both VigiCrue and CTRIP upstream forcings, the assimilation of in-situ observations only in IDA as well as the joint assimilation of in-situ water level and RS-derived WSR observations in IGDA leads to a significant improvement in reduced RMSE values. Indeed, the gain with respect to FR amounts to 65.15% when using observed inflow discharge and 88.69% when using CTRIP discharge for $IGDA^C$, with very similar results for IDA^C. The RMSEs at observing stations from the CTRIP-forced experiment $IGDA^C$ remain slightly larger (14-17 cm) than those of the simulations forced by VigiCrue discharges (7-9 cm). This demonstrates that the assimilation of in-situ data efficiently constrain the assimilation algorithm.

Table 1: Water level RMSE computing at observing stations with respect to observed WSE for 2021 flood event for FR^V, IDA^V, $IGDA^V$, FR^C, IDA^C and $IGDA^C$

RMSE [m]	Tonneins	Marmande	La Réole	Gain
FR^V	0.106	0.392	0.536	-
IDA^V	0.062	0.071	0.081	69.43%
$IGDA^V$	0.073	0.074	0.090	65.15%
FR^C	1.209	1.405	1.598	-
IDA^C	0.160	0.148	0.130	89.37%
$IGDA^C$	0.166	0.160	0.141	88.69%

c. Results in the observation space with 2D metrics on flood extent over the simulation domain, using with contingency maps and Critical Success Index (CSI)

The merits of assimilating WSR in addition to in-situ data, is significant in the floodplain. The contingency map between the simulated flood extent and the observed flood extent derived from Sentinel-1 is computed and displayed in Figure 8. It indicates for each pixel within the studied catchment if the simulation leads to a True Positive (*TP*) or a True Negative (*TN*) (respectively, if a pixel is correctly predicted as flooded or correctly identified as non-flooded according to the Sentinel-1-derived flood extent maps), or if it fails as being a False Positive (*FP*) or a False Negative (*FN*) (respectively, if a pixel is not correctly predicted as flooded or not correctly predicted as non-flooded). The CSI, also called Threat Score, computes the ratio between the number of *TP* over the sum pixels of *TP, FP*, and *FN*. A CSI close to 100% indicates a perfect result with respect to the reference (here S1-derived flood extents).

At the flood peak on 03/02/2021 (top panel), both FR experiments show many large areas of underpredicted flooding (shown by yellow areas), with FR^C being the more severe case due to CTRIP providing much less inflow discharge. These underprediction areas are significantly reduced by the DA for both $IGDA^V$ and $IGDA^C$. It should be noted that the assimilation of in-situ only data in IDA^V and IDA^C brings an improvement with respect to FR but significant underprediction, especially when CTRIP forcing is used. This demonstrates that the assimilation of WSR and the associated correction

of the hydraulic state in the subdomains of the floodplain brings further improvement with respect to the in-situ only IDA strategy. Regarding the use of Vigicrue or CTRIP forcing, the CSI computed for $IGDA^C$ despite the underestimation of flood peak discharge by CTRIP still manages to reach the same level as the $IGDA^V$. Indeed, DA significantly improves the CSI score for both experiments with VigiCrue and CTRIP forcing, with almost the same resulting score of 68%.

During the flood recess on 07/02/2021 (bottom panel), both FR experiments tend to over-predict flooding (shown by red areas) as the model struggles to empty the floodplain after the flood peak. The assimilation of in-situ data in IDA tends to even degrade the results in the floodplain and the assimilation of S1-derived WSR is all the more visible. DA significantly reduces these areas, especially thanks to the correction of the water level in subdomains of the floodplain dH_k with $k \in [1, 5]$. With such a reduction, the CSI score is shown to be improved between the two VigiCrue experiments. Regarding the experiments with the CTRIP discharge, it can be noted that the CSI of $IGDA^C$ (32.17%) during the flood recession is even lower than that of FR^C (35.31%). This is due to the aforementioned lack of inflow discharge throughout the event, and thus this results in the water extent remaining small at flood recess, despite the model's error related to the lack of physical process for water evacuation. Such an assessment should be made alongside with the 1D assessment for the same experiments (RMSEs by $IGDA^C$ reduced by 73.69% compared to FR^C). A similar CSI at this date between $IGDA^V$ and $IGDA^C$, respectively 32.60% and 32.17%, likely shows the ceiling limit of the DA strategy and T2D model, regardless of the used inflow discharge. This also advocates for further improvement of the model physical processes regarding infiltration and evapotranspiration parameters (outside of the DA).

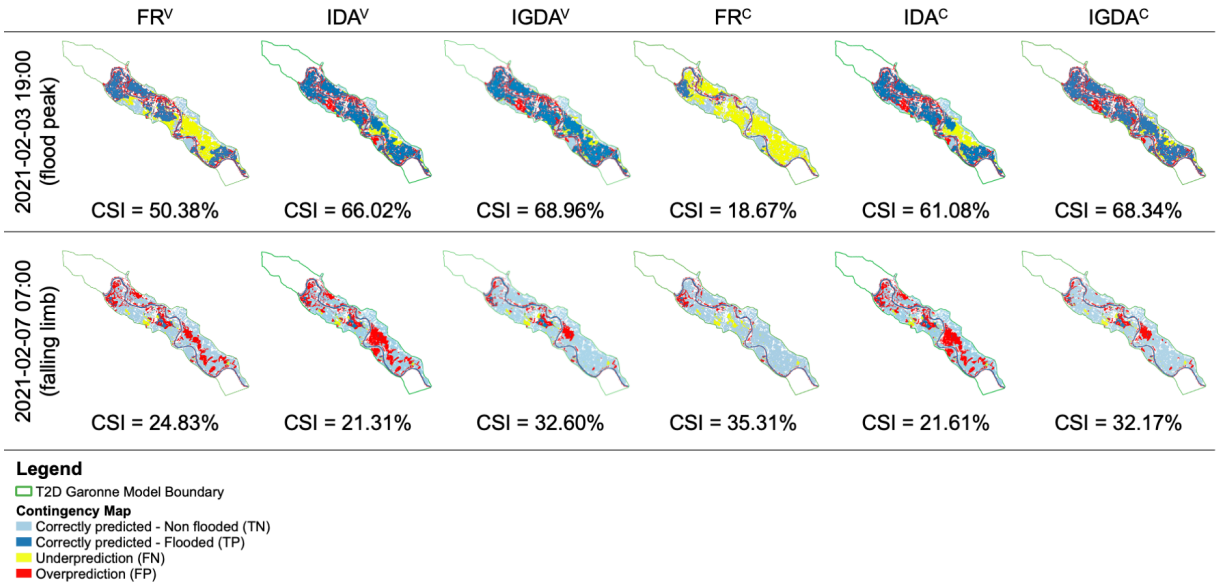

Figure 8: Contingency maps and CSI computed between simulated flood extents and S1-derived observed flood extents for FR^V, IDA^V, $IGDA^V$, FR^C, IDA^C and $IGDA^C$ at the flood peak and at recess time for the 2021 flood event.

5. Conclusion and perspectives

This study presents the merits of assimilating 2D flood extent observations derived from Sentinel-1 SAR images with an EnKF implemented on the 2D hydraulic model TELEMAC-2D, focusing on a

major flood event in 2021 over a subdomain of the Garonne catchment near Marmande, using a Gaussian Anamorphosis function to deal with non-Gaussian SAR-derived observation errors, jointly with in-situ water level observations. The flood extent observations are expressed in terms of WSR computed over defined sensitive subdomains of the floodplain. Six experiments were carried out both in Free Run and Data Assimilation mode, using upstream forcing data that are either observed discharges from an observing station in the VigiCrue network, or discharges simulated by a large-scale hydrologic model ISBA-CTRIP. The control vector gathers friction coefficient and forcing correction, and is augmented with correction of the hydraulic state in subdomains of the floodplains. It was shown that DA greatly improves the water level in the river bed and the representation of the dynamics of the flow in the floodplain, using 1D and 2D metrics. While the assimilation of in-situ data allows to correct the hydraulic state in the river bed, the assimilation of WSR allows to correct the dynamics of the flow in the flood plain, especially at flood peak and during recess.

The experimental setting allows to show that the DA algorithm succeeds in identifying corrections to the friction coefficients and the hydrologic forcings so that the simulated hydraulic state is coherent with the assimilated in-situ and RS observations. This demonstrates the merits of assimilating joint in-situ and remote sensing data for re-analysis of past flood events. The complementarity of in-situ and RS sensing data was highlighted. This study also provides a more accurate hydraulic state, from which a forecast (or an ensemble of forecasts) can start. This will be achieved in future work. The stationarity of the correction identified over a DA cycle, beyond the end of the cycle (the present time) should be investigated. While the validation of the DA results with respect to independent data was assessed in synthetical experiments (not shown), this strategy remains difficult for real events due to the scarcity of the observing network in time and/or space.

This work also demonstrates that while imperfect, forcing data provided by a hydrologic model can be efficiently used as input to a local hydraulic model and that DA allows for an efficient reduction of the uncertainty in such hydrology products. These findings advocate for a multi-source strategy for the assimilation algorithm implemented on top of a chained hydrology-hydraulic model that is favorable for short term as well as for extended lead time forecasts, especially in poorly-gauged or ungauged catchments.

Acknowledgments

The authors gratefully thank Electricité de France (EDF) for providing the TELEMAC-2D model on the Garonne Downstream catchment, and the SCHAPI, SPCs Garonne-Tarn-Lot and Gironde-Adour-Dordogne for providing in-situ data. They also would like to thank E. Simon (IRIT) for fruitful discussions and advice concerning the Gaussian anamorphosis.

REFERENCES

Dasgupta, A., Hostache, R., Ramsankaran, R. A. A. J., Grimaldi, S., Matgen, P., Chini, M., ... & Walker, J. P. (2021). Earth observation and hydraulic data assimilation for improved flood inundation forecasting. In *Earth observation for flood applications* (pp. 255-294). Elsevier, https://doi.org/10.1016/B978-0-12-819412-6.00012-2

Decharme B., Delire C., et al., 2019. Recent changes in the ISBA‐CTRIP land surface system for use in the CNRM‐CM6 climate model and in global off‐line hydrological applications. *Journal of Advances in Modeling Earth Systems, 11*(5): 1207-1252, https://doi.org/10.1029/2018MS001545

Decharme B., Alkama R., Papa F., Faroux S., Douville H., and Prigent C., 2012. Global Off-line Evaluation of the ISBA-TRIP Flood Model. *Climate Dynamics, 38*(7): 1389-1412. https://doi.org/10.1007/s00382-011-1054-9

EMDAT, Disasters in numbers, 2021. Technical report Centre for Research on the Epidemiology of Disasters Institute Health and Society – UCLouvain. RT-0300, CRED. https://cred.be/sites/default/files/2021_EMDAT_report.pdf

Garambois, P. A., Larnier, K., Monnier, J., Finaud-Guyot, P., Verley, J., Montazem, A. S., & Calmant, S. (2020). Variational estimation of effective channel and ungauged anabranching river discharge from multi-satellite water heights of different spatial sparsity. *Journal of hydrology*, *581*, 124409, https://doi.org/10.1016/j.jhydrol.2019.124409

Grimaldi, S., Li, Y., Pauwels, V. R., & Walker, J. P. (2016). Remote sensing-derived water extent and level to constrain hydraulic flood forecasting models: Opportunities and challenges. *Surveys in Geophysics*, *37*, 977-1034, https://doi.org/10.1007/s10712-016-9378-y

Hostache, R., Chini, M., Giustarini, L., Neal, J., Kavetski, D., Wood, M., ... & Matgen, P. (2018). Near‐real‐time assimilation of SAR‐derived flood maps for improving flood forecasts. *Water Resources Research*, *54*(8), 5516-5535, https://doi.org/10.1029/2017WR022205

Martinis, S., Kuenzer, C., & Twele, A. (2015). Flood studies using synthetic aperture radar data. In *Remote Sensing of Water Resources, Disasters, and Urban Studies* (pp. 145-173). CRC Press, https://doi.org/10.1201/b19321

Munier S., Decharme B., 2022. River network and hydro-geomorphological parameters at 1/12° resolution for global hydrological and climate studies. *Earth System Science Data, 14*(5): 2239-2258, https://doi.org/10.5194/essd-14-2239-2022

Nguyen T. H., Ricci S., Fatras C., Piacentini A., Delmotte A., Lavergne E., Kettig P., 2022a. Improvement of Flood Extent Representation with Remote Sensing Data and Data Assimilation. *IEEE Transactions on Geoscience and Remote Sensing, 60*(Art no. 4206022): 1-22, https://doi.org/10.1109/TGRS.2022.3147429

Nguyen T. H., Ricci S., Piacentini A., Fatras C., Kettig P., Blanchet G., ..., Baillarin S., 2022b. Dual State‐Parameter Assimilation of SAR-derived Wet Surface Ratio for Improving Fluvial Flood Reanalysis. *Water Resources Research*, 58, e2022WR033155. https://doi.org/10.1029/2022WR033155

Nguyen T. H., Ricci S., Piacentini A., Simon E., Rodriguez Suquet R., and Peña Luque S., 2023. Gaussian Anamorphosis for Ensemble Kalman Filter Analysis of SAR-Derived Wet Surface Ratio Observations, *arXiv preprint* arXiv:2304.01058, https://arxiv.org/abs/2304.01058

Noilhan J., Planton S., 1989. A simple parameterization of land surface processes for meteorological models. *Monthly Weather Review, 117*(3): 536-549, https://doi.org/10.1175/1520-0493(1989)117<0536:ASPOLS>2.0.CO;2

Oki T., Sud Y. C., 1998. Design of Total Runoff Integrating Pathways (TRIP)—A global river channel network. *Earth interactions, 2*(1): 1-37, https://doi.org/10.1175/1087-3562(1998)002%3C0001:DOTRIP%3E2.3.CO;2

Revilla-Romero, B., Wanders, N., Burek, P., Salamon, P., & de Roo, A. (2016). Integrating remotely sensed surface water extent into continental scale hydrology. *Journal of hydrology*, *543*, 659-670, https://doi.org/10.1016/j.jhydrol.2016.10.041

Simon E., Bertino L., 2012. Gaussian anamorphosis extension of the DEnKF for combined state parameter estimation: Application to a 1D ocean ecosystem model. *Journal of Marine Systems, 89*(1): 1-18, https://doi.org/10.1016/j.jmarsys.2011.07.007